Cutting temperatures in milling operations of difficult-to-cut materials

Mohsen Soori, Mohammed Asmael

Journal of New Technology and Materials (JNTM)
J. New Technol. Mater.
Vol. 11, N°01 (2021)47-56

OEB Univ. Publish. Co.

Cutting temperatures in milling operations of difficult-to-cut materials

Mohsen Soori * and Mohammed Asmael

Department of Mechanical Engineering, Eastern Mediterranean University, Famagusta, North Cyprus, Via Mersin 10, Turkey

* Corresponding author, email: mohsen.soori@gmail.com, mohsen.soori@emu.edu.tr

Received date: May 05, 2021 ; revised date: June 12, 2021 ; accepted date: June 15, 2021

Abstract

Due to high strength-to-weight ratio and corrosion resistance, difficult-to-cut materials are used in the aerospace, automotive and medical industries. High mechanical and thermal loading occur during machining operations of difficult-to-cut materials, reducing cutting tool life and machining process performance. So, analyzing the cutting temperatures in milling operations of difficult-to-cut materials can increase the efficiency in production process of the parts from the alloys. Application of the virtual machining system is developed in the study to predict the cutting temperature during machining operations of difficult-to-cut materials such as Inconel 718, Titanium alloy Ti6Al4V and Nickel-base superalloy gH4133B. The modified Johnson–Cook model is used to analyze the coupled effects of strain rate and deformation temperature on flow stress during milling operations of the alloys. The finite element simulation of the milling operations is implemented for the alloys in order to obtain the cutting temperature of the cutting tool and workpiece during chip formation process. To validate the study, the experimental results are compared to the finite element results obtained from the virtual machining system. As a result, the study can provide an effective device in terms of efficiency enhancement of machining operations by analyzing and decreasing the cutting temperature in milling operation of difficult-to-cut materials.

Keywords: Cutting Temperature; Difficult to Cut Materials; Modified Johnson–Cook model; Virtual Machining

1. Introduction

The applications of hard-to-cut materials in aerospace industries, aeronautics, automotive and medical instruments are due to the metals' unique properties such as High strength-to-weight ratio, corrosion resistance, low thermal expansion and high hardness. Because of its light weight and high strength, titanium 6Al-4V is the most commonly used material in aerospace industries. Inconel 718 is used to make significant parts of aircraft turbojet engines, such as disks, blades, and casing for the high-pressure part of the compressor, as well as discs and blades for turbines. Implants (artificial joints, dental-use) and trauma and surgical instruments are produced from difficult-to-machine materials like titanium alloys, stainless alloys, and nickel-base superalloy account for 80% of the production for machined components in the medical equipment industry. Because of their low thermal conductivity and heat resistance, these alloys are difficult to machine. So, machining operations on difficult-to-cut materials result in high mechanical and thermal loading, reducing cutting tool life and high manufacturing cost. As a result, analyzing and decreasing cutting temperature in milling operations of difficult-to-cut materials can increase efficiency in machining operations of the alloys by providing higher material removal rates with longer cutting tool life.

A new cryogenic cooling approach is presented by Bagherzadeh and Budak [1] to in order to increase efficiency in milling operations of the difficult-to-cut materials. To analyze and decrease cutting temperatures and increase cutting tool life during milling operations of difficult to cut materials, advanced cooling system is presented by Shokrani and Betts [2]. To optimize machining parameters to minimize cutting force and temperature during turning of difficult to cut materials, application of taguchi method is presented by Struzikiewicz et al. [3]. To decrease cutting temperature in machining operations of difficult-to-cut materials, application of the internally cooled cutting tools is investigated by Isik [4]. To increase productivity in machining operations of difficult-to-cut materials, a review of recent developments is presented by Pandey and Datta [5]. To analyze cutting temperature in machining operations of titanium alloy Ti6Al4V, effects of cutting conditions as up-milling and down-milling on the milling process is presented by Wo and Zhang [6]. To predict and analyze cutting temperature in orthogonal cutting of Ti6Al4V, analytical model of cutting temperature is developed by SHAN et al. [7]. To analyze and decrease the cutting temperatures in terms of efficiency enhancement of machining operations, investigation of cutting temperature during turning Inconel 718 is

presented by Zhao et al. [8]. To measure and decrease the cutting temperature in turning Inconel 718, advanced measurement method using an improved two-color infrared thermometer is presented by Zhao et al. [9]. The tool-chip heat partition coefficient and cutting temperature during orthogonal machining operations of inconel 718 is investigated by Zhao et al. [10] to study the effects of PVD AlTiN coated cutting tool to the chip formation process. To increase efficiency in machining operations of hard to cut materials, effects of nano-cutting fluids on tool performance and chip morphology during machining Inconel 718 is studied by Hegab et al. [11]. Machinability in heat-assisted machining of nickel-base alloy is studied by Parida et al. [12] to decrease machining power, tool wear and specific cutting energy in machining operations of difficult to cut materials. Numerical analysis of chip geometry on hot machining of nickel base alloy is presented by Parida and Maity [13] to analyze the machining operations of hard to cut materials.

To analyze and modify the machining operations in virtual environments, virtual machining systems and applications is presented by Soori et al. [14-17]. In order to analyze and increase efficiency in process of part production using welding operation, a review in recent development of friction stir welding operations is presented by Soori et al. [18]. Mechanical behavior of materials in metal cutting operations is reviewed by Soori and Asmael [19] to analyze the cutting temperate, material removal rate, workpiece deformation and residual stress during machining operations.

Virtual machining systems in milling and turning CNC machine tools is reviewed by Soori and Arezoo [20] to develop the applications of virtual machining systems in part production process. To increase accuracy and reliability of machined turbine blades, virtual minimization of residual stress and deflection errors in five-axis CNC milling operations of turbine blades is presented by Soori and Asamel to [21]. To increase accuracy as well as efficiency in process of part production, virtual simulation of machining and grinding processes along the NC tool path is presented by Altintas et al. [22]. To predict the dynamic behavior in laser additive manufacturing of FeCr alloy, a comparative study on Johnson-Cook and modified Johnson-Cook constitutive material model is presented by Zhao et al. [23]. Finite element analysis procedure for porous structures is developed by De Galarreta et al. [24] to increase accuracy in simulation and analysis of lattice structures. To increase cutting tool life in machining operations of difficult-to-cut materials, cutting temperature and cutting tool wear are measured and analyzed by Karaguzel et al. [25].

The cutting temperatures during chip formation process and machining operations are analyzed in different research works in order to be minimized. According to the analysis of previous published papers, the area of cutting temperature prediction in machining operations of difficult to cut materials by using virtual machining systems is not studied.

In this study, application of virtual machining systems is developed in order to predict cutting temperatures during machining operations of difficult to cut materials such as Inconel 718, Titanium alloy Ti6Al4V and Nickel-base superalloy gH4133B. The coupled effects of strain rate and deformation temperature on flow stress during milling operations of alloys are investigated using a modified Johnson–Cook model. In order to determine the cutting temperature of the cutting tool and workpiece during the chip forming process, a Finite Element Method (FEM) simulation of milling operations is implemented for alloys. To validate the study, the experimental results are compared to the finite element results obtained from the virtual machining system.

In the section 2, the cutting force modelling method is described. The Johnson–Cook model and modified Johnson–Cook model for the Inconel 718, Titanium alloy Ti6Al4V and Nickel-base superalloy gH4133B are presented in the section 3. The developed virtual machining system to predict the cutting temperature is described in the section 4. To simulate and validate the proposed method in the study, finite element simulation and experimental method is presented in section 5. Finally, the obtained results of the study is presented in the section 6.

2. Cutting Force Model

The In this study, the cutting force method introduced by Engin and Altintas [26] was used to calculate the cutting forces along machining paths. This model's equations can be parametrically described for various helical end mills. Cutting force equations for any kind of cutting tool can be obtained by substituting values for the parameters based on tool envelop geometry. Figure 1 [26] depicts a typical milling process with a general end mill cutting tool.

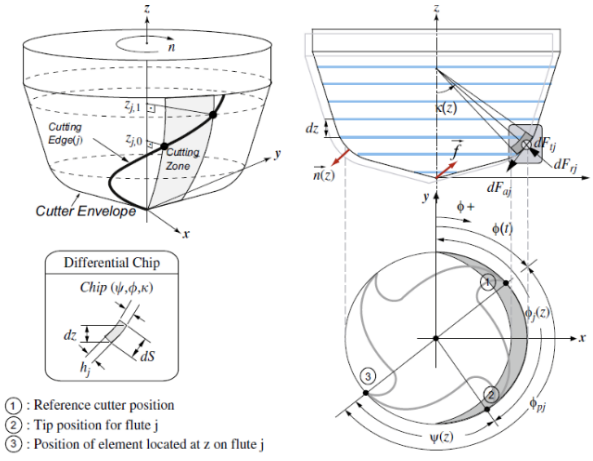

Figure 1. Mechanics and kinematics of three-axis milling [26].

Where $\phi_{pj}$is pitch angle of flute j, $\phi_j(z)$ is total angular rotation of flute j at level z on the XY plane, $\psi(z)$ is radial lag angle and $\kappa(z)$ is axial immersion angle. In the

differential chip, $dz$is differential height of the chip segment, $ds$is the length of cutting edge and $h_j$is height of valid cutting edge from tool tip. Thus, Eq. (1) shows the differential tangential(dF_t), radial (dF_r) and axial(dF_a) cutting forces acting on an infinitely small cutting-edge section.

$$\begin{cases} dF_t = K_{te}ds + K_{tc}h(\phi_j,k)db \\ dF_r = K_{re}ds + K_{rc}h(\phi_j,k)db \\ dF_a = K_{ae}ds + K_{ac}h(\phi_j,k)db \end{cases} \quad (1)$$

Where $h(\phi_j,k)$ is the uncut chip thickness normal to the cutting edge and varies with the position of the cutting point and cutter rotation.

The uncut chip thickness in a flat end milling operation can be calculated using Eq. (2) [27].

$$h(\phi_j,k) = S_{tj}Sin(\phi_j) \quad (2)$$

Where $S_{tj}$and $\phi_j$are feed per tooth and radial lag angle of tooth j respectively.

In the direction of the cutting velocity, db is the estimated length of an infinitesimal cutting flute, which can be seen as Eq (3).

$$db = \frac{dz}{SinK} \quad (3)$$

The edge cutting coefficients K_{te},$K_{re}$and K_{ae} are constants which are proportional to the cutting-edge length ds.

Shear and edge force components are represented by sub-indices (c) and (e), respectively. The sheer force coefficients K_{tc},K_{rc} and K_{ac} can be obtained from milling experiments [28]. To confirm the current study, an experimental operation was used to obtain edge cutting and sheer force coefficients. The geometric model is used to determine the cutting point locations along the flute. The rigid body kinematics as well as structural displacements of the cutter and workpiece are used to locate the same flute point on the cut surface. After the chip load has been calculated and the cutting coefficients for the local edge geometry have been determined, the cutting forces in the Cartesian coordinate system can be determined using Eq (4).

$$\begin{bmatrix} dF_x \\ dF_y \\ dF_z \end{bmatrix} = \begin{bmatrix} -\sin\phi_j \sin\kappa & -\cos\phi_j & -\sin\phi_j \cos\kappa \\ -\cos\phi_j \sin\kappa & \sin\phi_j & -\cos\phi_j \cos\kappa \\ \cos\kappa & 0 & -\sin\kappa \end{bmatrix} \begin{bmatrix} dF_r \\ dF_t \\ dF_a \end{bmatrix} \quad (4)$$

The total cutting forces for the rotational position ϕ_j can be found by integrating as Eq. (5).

$$\begin{aligned} F_x(\phi_j) &= \sum_{j=1}^{N_f} F_{xj}[\phi_j(z)] \\ &= \sum_{j=1}^{N_f} \int_{Z_1}^{Z_2} [-dF_{rj}\sin\phi_j \sin\kappa_j \\ &\quad - dF_{tj}\cos\varphi_j - dF_{aj}\sin\phi_j \cos\kappa_j] dz \\ F_y(\phi_j) &= \sum_{j=1}^{N_f} F_{yj}[\phi_j(z)] \\ &= \sum_{j=1}^{N_f} \int_{Z_1}^{Z_2} [-dF_{rj}\cos\phi_j \sin\kappa_j \\ &\quad + dF_{tj}\sin\phi_j - dF_{aj}\cos\phi_j \cos\kappa_j] dz \\ F_z(\phi_j) &= \sum_{j=1}^{N_f} F_{zj}[\phi_j(z)] \\ &= \sum_{j=1}^{N_f} \int_{Z_1}^{Z_2} [dF_{rj}\cos\kappa_j \\ &\quad - dF_{aj}\sin\kappa_j] dz \end{aligned} \quad (5)$$

Where N_f is the number of flutes on the cutter, $z_1$and $z_2$are the contact boundaries of the flute which is in the cut and κ_j is axial immersion angle of flute j.

In the flat end mill the κ = 90°, thus the cutting force of Eq. (5) can be simplified as Eq. (6)

$$h(\phi_j,k) = S_{tj}Sin(\phi_j)Sin(k_j) \quad (6)$$

WhereS_{tj}, ϕ_j and $\kappa_j$are feed per tooth, radial lag angle and axial immersion angle of tooth j respectively.

$$\begin{cases} dF_x(\phi_j) = -dF_t\cos\phi_j - dF_r\sin\phi_j \\ dF_y(\phi_j) = +dF_t\sin\phi_j - dF_r\cos\phi_j \\ dF_z(\phi_j) = +dF_a \end{cases} \quad (7)$$

3. Johnson–Cook model

The Johnson–Cook model is widely implemented to describe the flow stress of a material as a function of strain, strain rate, and temperature effects because of its high accuracy and mathematical simplicity. Individual effects of strain hardening, strain rate hardening, and thermal softening on the flow stress of the material undergoing

deformation are represented by the three terms. Due to its suitability for use in FE codes, it has become widely used to characterize the material deformation behavior of various materials. The Johnson–Cook model is presented as Eq. (8) [29].

$$\sigma = (A + B\varepsilon^{n})(1 + C ln\frac{\dot{\varepsilon}}{\dot{\varepsilon 0}})\left[1 - \left(\frac{T-T_0}{T_m-T_0}\right)^{m}\right] \quad (8)$$

where ε is the equivalent plastic strain˙ andε˙0 are the equivalent and reference plastic strain rates, T, T_m, and T_0 are the material's cutting zone, melting, and room temperature, respectively. N is the strain hardening index and m is the thermal softening index. Also, And A, B, and C represent the yield strength, strain, and strain rate sensitivities of the material, respectively.

The Johnson–Cook model, does not consider the aggregation effect of any influence factor, but instead assumes that the three influencing factors of strain, strain intensity, and temperature are mutually independent. Such strain rate dependence is impossible to forecast using the traditional J–C constitutive model. As compared to the original Johnson–Cook model, the improved Johnson–Cook model considers the coupled effects of strain rate and deformation temperature on flow stress, significantly improving the model's prediction accuracy [30].

Lin et al. [31] propose an updated Johnson–Cook model to solve the Johnson–Cook model's limitations as Eq. (9),

$$\sigma = (A_1 + B_1\varepsilon + B_2\varepsilon^{2})(1 + C_1 ln\dot{\varepsilon})exp\left[(\lambda_1 + \lambda_2 ln\dot{\varepsilon})(T - T_{ref})\right] \quad (9)$$

where A_1, B_1, B_2, C_1, λ_1 and λ_2 are material constants, and the meanings of the other parameters are the same as that in the Johnson–Cook model.

The dynamic behavior and a modified Johnson–Cook model of Inconel 718 at high strain rate and elevated temperature is presented by Wang et al. [32] as Eq. (10),

$$\sigma = (963 + 937\varepsilon^{0.333})(1 + C ln\frac{\dot{\varepsilon}}{\dot{\varepsilon 0}})(1 - (\frac{T-20}{1300})^{1.3}) \quad (10)$$

Where C can be obtained by Eq. (11),

$$C = 0.0232 - (0.00372 + 0.0021\sin\left(\frac{\dot{\varepsilon}-5000}{3000}\pi\right))\sin(\frac{T-500}{150}\pi) \quad (11)$$

The firefly algorithm is used by Ren et al. [33] in order to present the modified Johnson–Cook model for cutting titanium alloy Ti6Al4V as Eq. (12),

$$\sigma = \left[724.7 + 683.1\varepsilon^{0.47}(\frac{1}{\exp(\varepsilon^{3.7758})})\right]\left[1 + 0.035\ln(\frac{\dot{\varepsilon}}{10^{-5}})\right]\left[1 - \left(\frac{T-293}{1584}\right)\right]\left[D + (1-D)(\tanh\left(\frac{1}{\varepsilon + P}\right))^{2.6195})\right] \quad (12)$$

Where D and P can be obtained by Eq. (13) and Eq. (14),

$$D = 1 - (\frac{T}{1877})^{0.9076} \quad (13)$$

$$P = (\frac{T}{1877})^{1.3247} \quad (14)$$

Wang et al. [34] present a modified Johnson-Cook definition of wide temperature and strain rate measured data on a nickel-base superalloy gH4133B as Eq. (15),

$$\sigma = (800 + 1500\varepsilon^{0.4})\left[1 + 0.0002ln\dot{\varepsilon} + 0.03(\frac{1}{11 - ln\dot{\varepsilon}} - \frac{1}{11})\right]\left\{1 - T^{1.4} + 0.3exp\left[-\frac{(T-T_p)^2}{51200}\right]\right\} \quad (15)$$

4. Virtual Machining System

To calculate cutting tool and predict the cutting temperatures in milling operations of difficult to cut materials, a virtual machining system is developed using the Visual Basic programming language. The module collects the nominal machining path, the geometry and material properties of the cutting tool, as well as the CAD model of the workpiece.

The developed virtual machining system can calculate cutting forces based on cutting tool information and machining process parameters. Cutting forces can thus be determined at each location of the cutting tool along machining paths.

The software is then connected to the Abaqus R2016X FEM analysis software to determine the cutting temperature as a result of machining operations. The workpiece's CAD model is then mesh generated in order to be analyzed by finite element methods. The modified Johnson–Cook model for the difficult to cut materials as Inconel 718, titanium alloy Ti6Al4V and nickel-base superalloy gH4133B are implemented in the finite element software to obtain the cutting temperature in the cutting tool as well as workpiece. Flowchart and strategy of the virtual machining system in cutting force calculation and cutting temperature prediction using virtual machining system is presented in the figure 2.

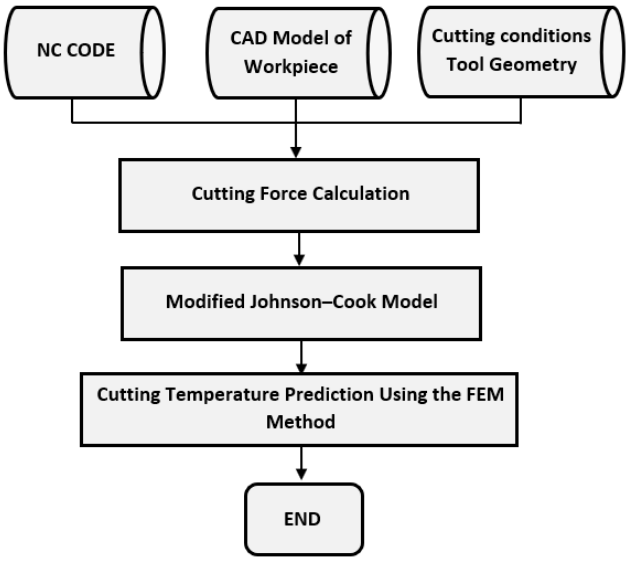

Figure 2. Flowchart and strategy of the virtual machining system in prediction of cutting force calculation and cutting temperature.

As a result, the virtual machining system in the study can predict the cutting temperature of the workpiece and cutting tool along machining paths.

5. Simulation and validation

In order to estimate the cutting coefficients for the Inconel 718, titanium alloy Ti6Al4V and nickel-base superalloy, the average cutting forces of twenty slot milling tests with 1.5 mm axial depth of cut have been measured by Kistler dynamometer. As a result, the cutting force coefficients for the Inconel 718 are as Eq. (16).

$$K_{tc} = 2190.54, K_{te} = 32.7$$
$$K_{rc} = 531.7, K_{re} = 41.9$$
$$K_{ac} = 742.98, K_{ae} = 6.2 \quad (16)$$

The cutting force coefficients for the titanium alloy Ti6Al4V are as Eq. (17).

$$K_{tc} = 1735.42, K_{te} = 24.9$$
$$K_{rc} = 380.31, K_{re} = 44.3$$
$$K_{ac} = 640.61, K_{ae} = 4.5 \quad (17)$$

The cutting force coefficients for the nickel-base superalloy gH4133B are as Eq. (18).

$$K_{tc} = 1849.7, K_{te} = 28.1$$
$$K_{rc} = 410.42, K_{re} = 39.2$$
$$K_{ac} = 680.4, K_{ae} = 5.7 \quad (18)$$

The machining parameters of the experiment are as 10,000 rpm spindle speed, cutting speed 30 m/min, feed 0.15 mm/rev, depth of cut 1.5 mm. The simulated cutting tool is 10 mm diameter 6 fluted Tungsten Carbide end mil. Finite element model of milling operation is simulated using the Abaqus R2016X FEM analysis software. To obtain the cutting temperature in slot milling operation, instantaneous cutting tool and workpiece temperature fields are simulated. For the simulations, a variable mesh density is used, with a minimum element size of 1 μm. A workpiece with chip geometry is meshed with 215,000 tetrahedral elements and a cutting tool end mill is meshed with 110,000 tetrahedral elements which are used in simulations of the milling process for complete immersion cutting. To achieve correct temperature distributions, the cutting area is meshed with an extra fine mesh. The finite element simulation of milling operation is shown in the figure 3.

The temperature distributions in the milling simulation of the Inconel 718 are obtained as Figure 4.

The temperature distributions in the cutting simulation of the Titanium alloy Ti6Al4V are obtained as Figure 5.

The temperature distributions in the cutting simulation of the Nickel-base superalloy gH4133B are obtained as Figure 6.

Experiments are performed on Inconel 718, Nickel-base superalloy gH4133B, titanium alloy Ti6Al4V, using cutting tool with 10 mm diameter, 6 fluted Tungsten Carbide end mill and 5-axis Kondia HM 1060 CNC machine tool. The K-type thermocouples with 130 μm diameter and 0.15 s response time are placed in the workpiece to measure the temperature of workpiece during milling operations. The comparison of simulation results and workpiece temperatures measured experimentally for the Inconel 718, Titanium alloy Ti6Al4V and Nickel-base superalloy gH4133B are shown in the figures 7, 8 and 9 respectively.

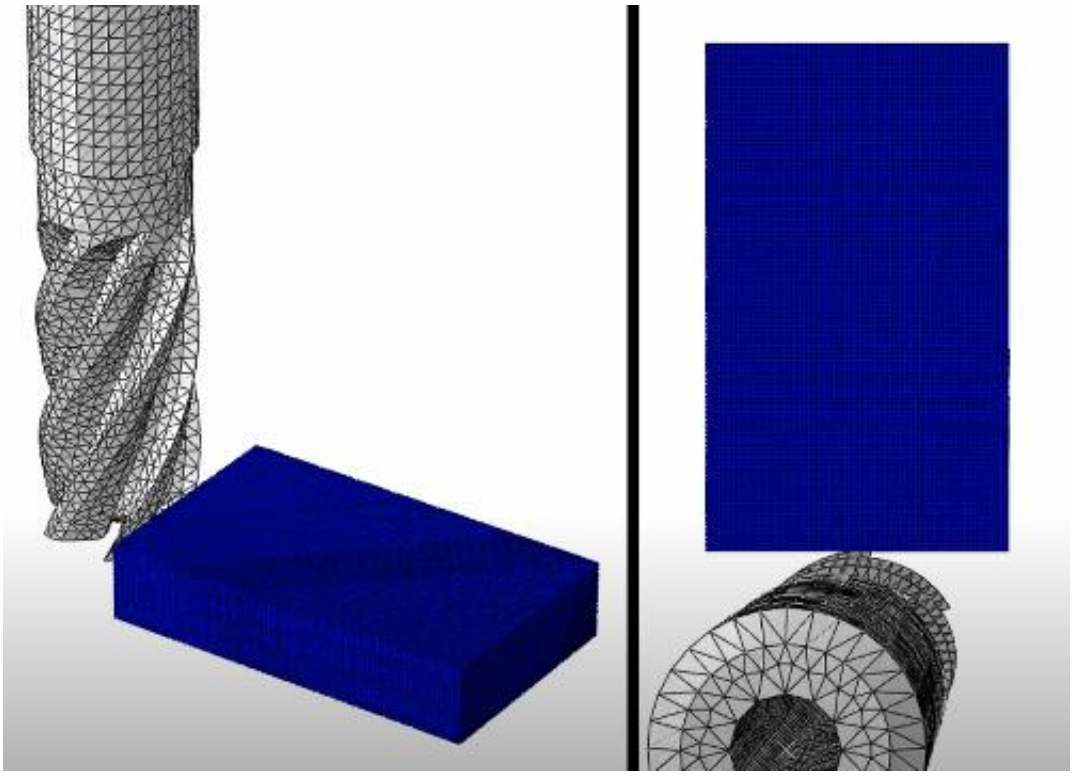

Figure 3. Finite element simulation of milling operation.

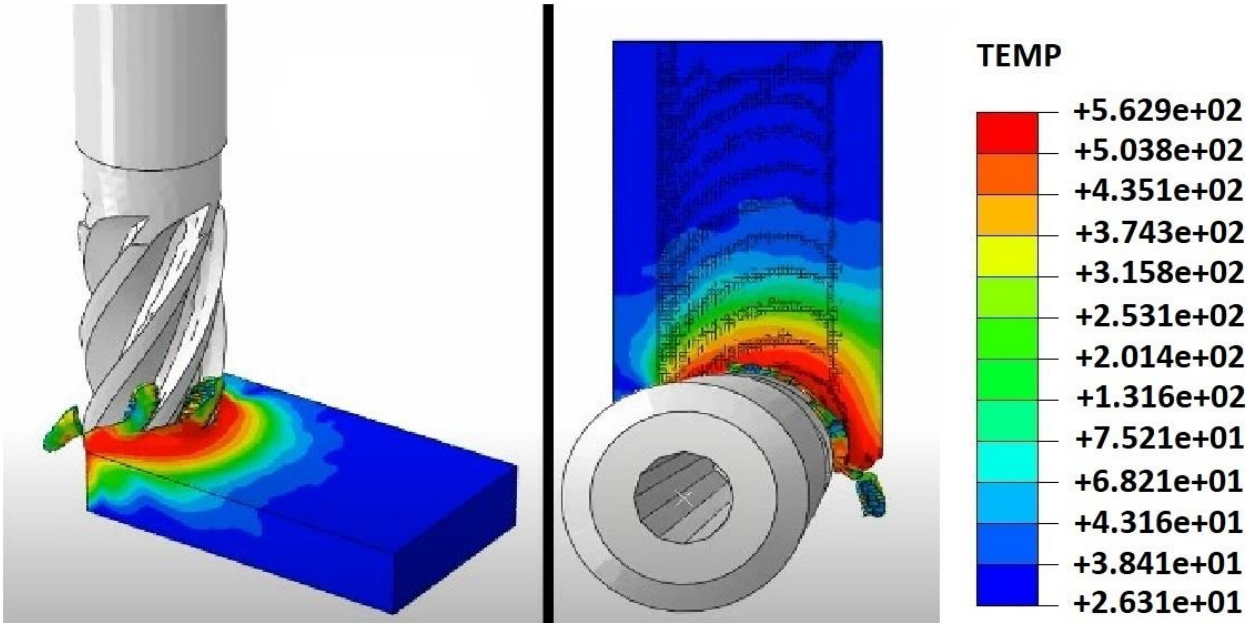

Figure 4. The temperature distribution in the milling simulation of the Inconel 718

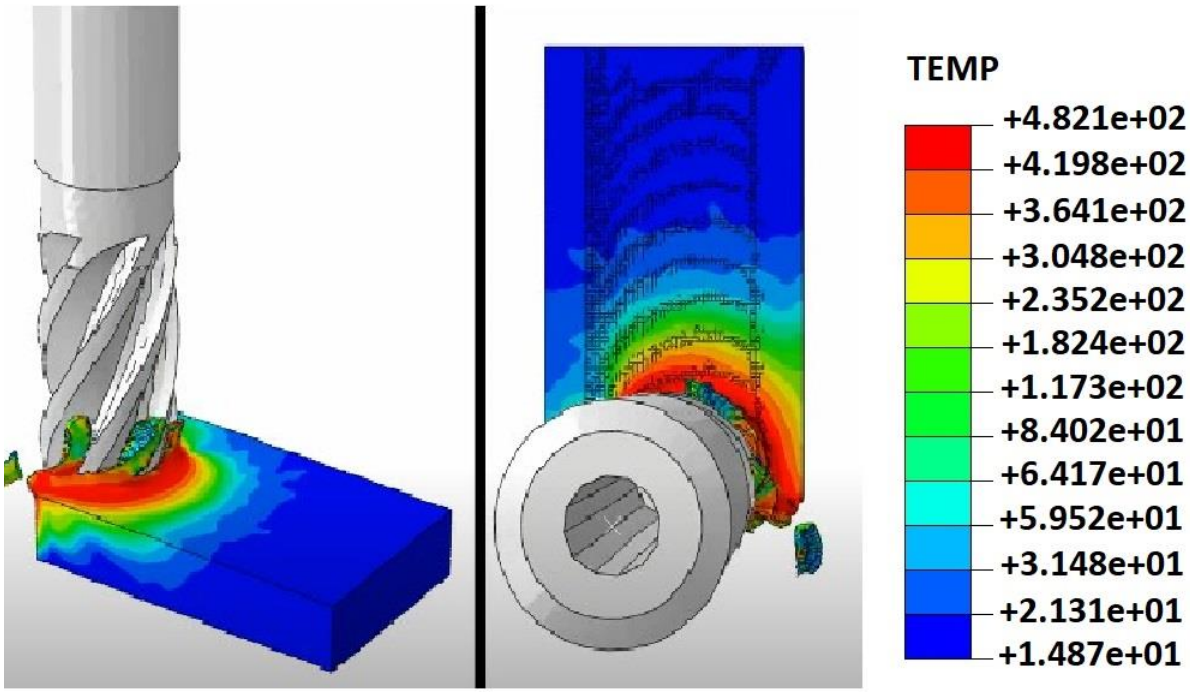

Figure 5. The temperature distribution in the milling simulation of the Titanium alloy Ti6Al4V.

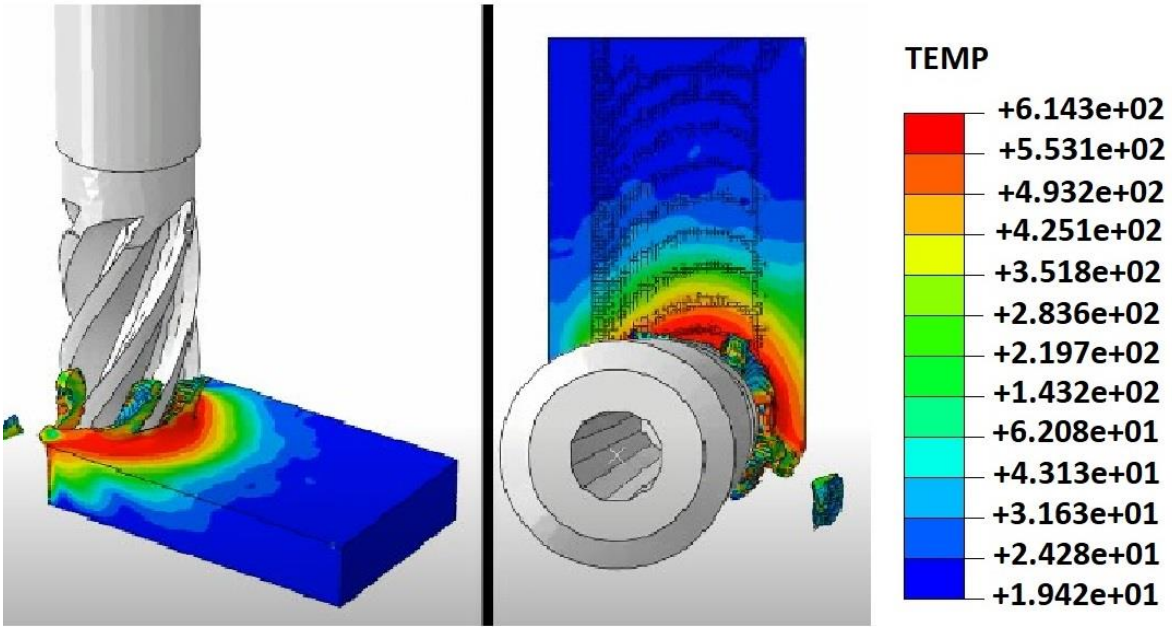

Figure 6. The temperature distribution in the milling simulation of the Nickel-base superalloy gH4133B.

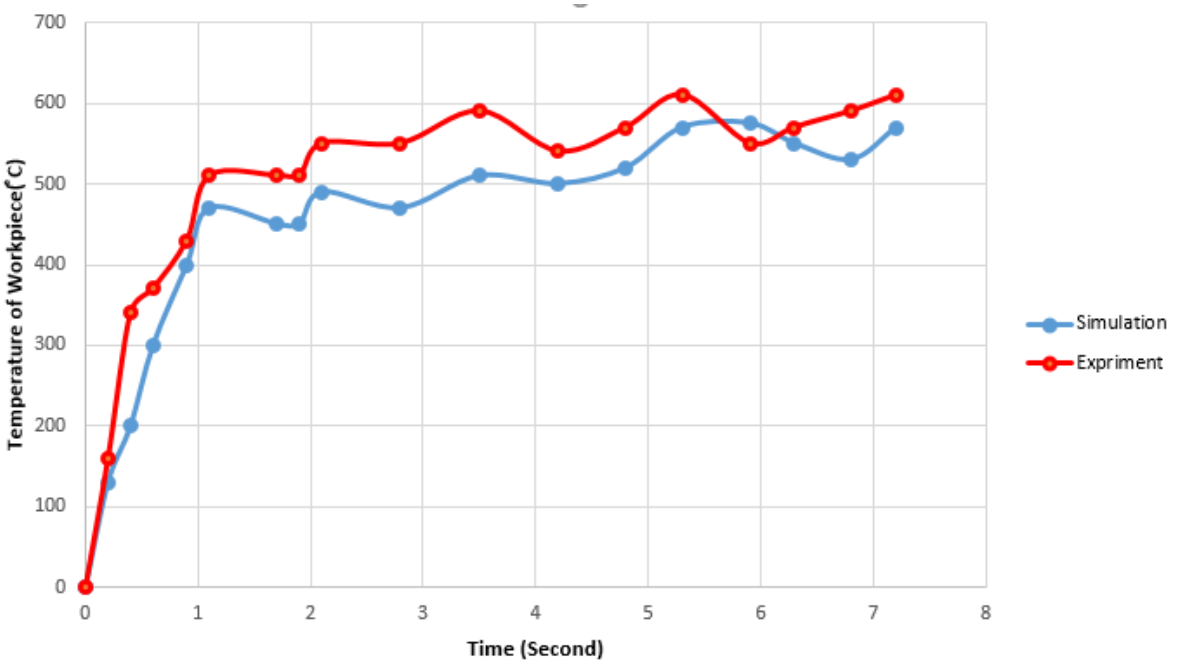

Figure 7. The simulation and workpiece temperatures measured experimentally for the Inconel 718.

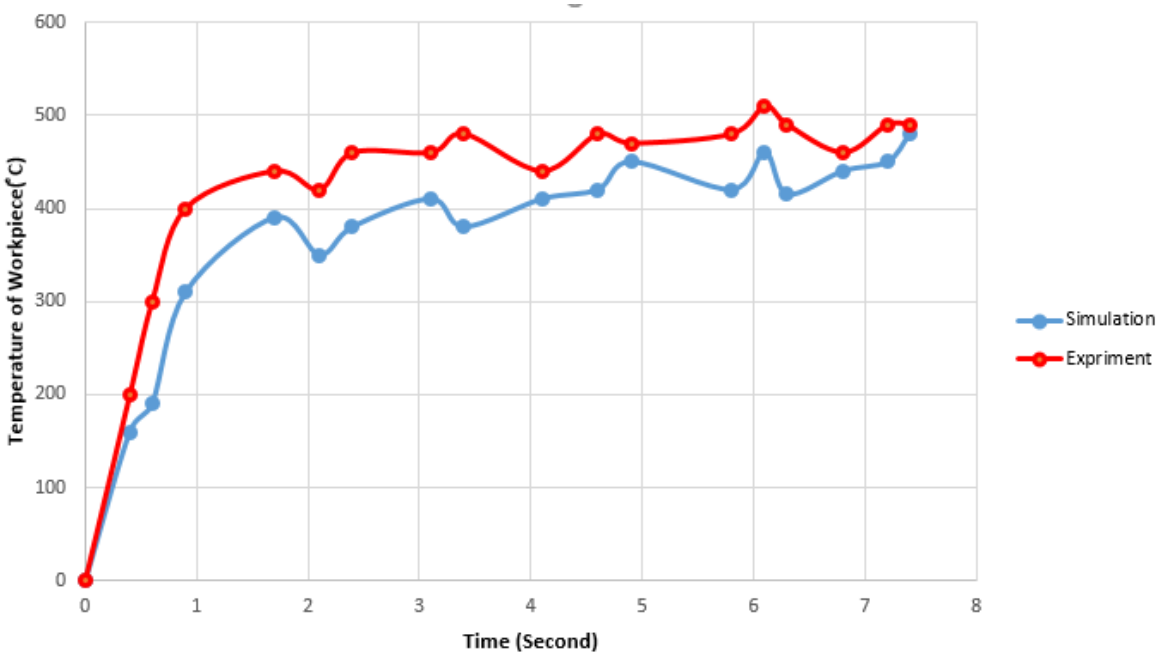

Figure 8. The simulation and workpiece temperatures measured experimentally for the Titanium alloy Ti6Al4V.

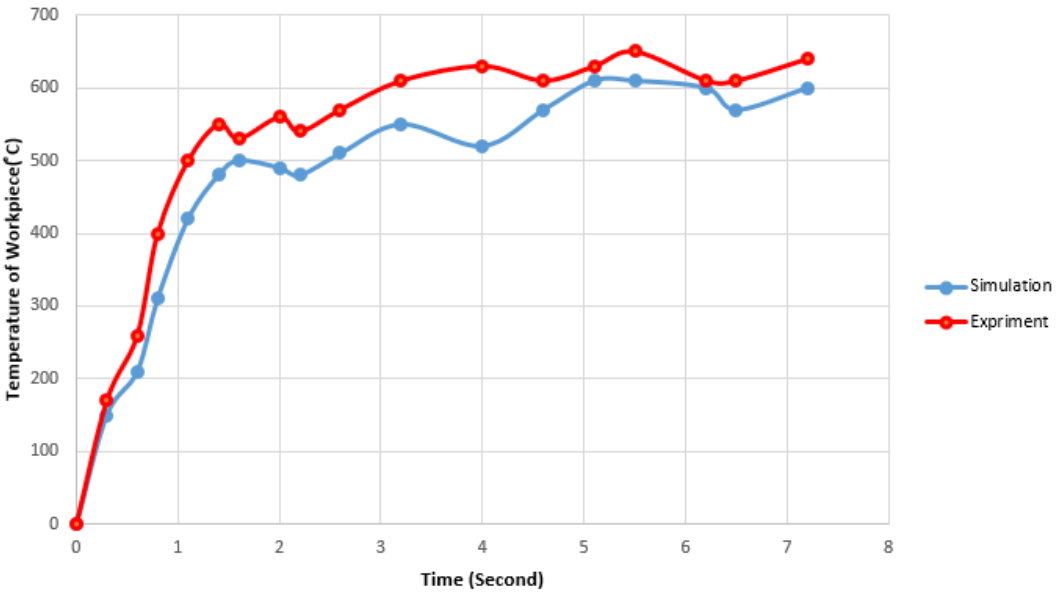

Figure 9. The simulation and workpiece temperatures measured experimentally for the Nickel-base superalloy gH4133B.

6. Conclusion

The materials with difficult to cut machining are used in different aerospace, automotive and medical industries due to high strength-to-weight ratio and corrosion resistance. High mechanical and thermal loading occur during machining operations on difficult-to-cut materials, decreasing cutting tool life and increasing production costs. As a result, analyzing and lowering the cutting temperature in milling operations of difficult-to-cut materials will improve the efficiency of alloy machining operations by allowing for higher material removal rates and longer tool life. Application of virtual machining system is developed in the study to predict the cutting temperature during milling operations of difficult to cut materials such as Inconel 718, Titanium alloy Ti6Al4V and Nickel-base superalloy gH4133B. The developed virtual machining system can accurately calculate the cutting forces along machining paths.

The modified Johnson–Cook Model is implemented in the study to simulate the chip formation process by considering the coupled effects of strain rate and deformation temperature on flow stress. The FEM method in then applied to the simulated milling operation in virtual environment to predict the cutting temperatures during chip formation process of difficult to cut materials. To validate the developed method in the study, experiments are performed on Inconel 718, Nickel-base superalloy gH4133B, titanium alloy Ti6Al4V using the 5-axis Kondia HM 1060 CNC machine tool. Then, the cutting temperature of workpiece and cutting tool are measured using the K-type thermocouples. As a result, good compatibilities are obtained in comparison of the simulated and experiment results of the cutting temperatures. The benefits of the developed virtual machining system can be the reduction of experimental testing and economic waste to analyze and decrease the cutting temperature during machining operations of difficult to cut materials. Moreover, the cooling effects and cutting tool wear conditions during machining operations of difficult to cut materials can be analyzed in order to increase efficiency in process of part production using machining operations. These are future concept of the author.

References

[1] A. Bagherzadeh, E. Budak, “Investigation of machinability in turning of difficult-to-cut materials using a new cryogenic cooling approach”, Tribol Int 119 (2018) 510-520.

[2] A. Shokrani, J. Betts, “A new hybrid minimum quantity lubrication system for machining difficult-to-cut materials”, CIRP Annals 69 (2020) 73-76.

[3] G. Struzikiewicz, W. Zębala, K. Rumian, “Application of Taguchi method to optimization of cutting force and temperature during turning of difficult to cut materials”, In: Key Engineering Materials, Trans Tech Publ, (2016) 114-118.

[4] Y. Isik, “Using internally cooled cutting tools in the machining of difficult-to-cut materials based on Waspaloy”, Adv Mech Eng 8 (2016) 1687814016647888.

[5] K. Pandey, S. Datta, “Hot machining of difficult-to-cut materials: A review”, Mater Today: Proceedings 44 (2021) 2710-2715.

[6] H. Wu, S. Zhang, “Effects of cutting conditions on the milling process of titanium alloy Ti6Al4V”, Int J Adv Manuf Technol 77 (2015) 2235-2240.

[7] S. Chenwei, X. Zhang, S. Bin, D. Zhang, “An improved analytical model of cutting temperature in orthogonal cutting of Ti6Al4V”, Chinese J Aeronaut 32 (2019) 759-769.

[8] J. Zhao, Z. Liu, Q. Shen, B. Wang, Q. Wang, "Investigation of cutting temperature during turning Inconel 718 with (Ti, Al) N PVD coated cemented carbide tools", Materials 11 (2018) 1281.
[9] J. Zhao, Z. Liu, B. Wang, Y. Hua, Q. Wang, "Cutting temperature measurement using an improved two-color infrared thermometer in turning Inconel 718 with whisker-reinforced ceramic tools", Ceramics Int 44 (2018) 19002-19007.
[10] J. Zhao, Z. Liu, B. Wang, J. Hu, "PVD AlTiN coating effects on tool-chip heat partition coefficient and cutting temperature rise in orthogonal cutting Inconel 718", Int J Heat Mass Transf 163 (2020) 120449.
[11] H. Hegab, U. Umer, M. Soliman, H.A. Kishawy, "Effects of nano-cutting fluids on tool performance and chip morphology during machining Inconel 718", The Int J Adv Manuf Technol 96 (2018) 3449-3458.
[12] A.K. Parida, K. Maity, "Study of machinability in heat-assisted machining of nickel-base alloy", Measurement 170 (2021) 108682.
[13] A.K. Parida, K. Maity, "Numerical analysis of chip geometry on hot machining of nickel base alloy", J Brazilian Soci Mech Sci Eng 40 (2018) 1-9.
[14] M. Soori, B. Arezoo, M. Habibi, "Accuracy analysis of tool deflection error modelling in prediction of milled surfaces by a virtual machining system", Int J Comput Appl Technol 55 (2017) 308-321.
[15] M. Soori, B. Arezoo, M. Habibi, "Virtual machining considering dimensional, geometrical and tool deflection errors in three-axis CNC milling machines", J Manuf Syst 33 (2014) 498-507.
[16] M. Soori, B. Arezoo, M. Habibi, "Dimensional and geometrical errors of three-axis CNC milling machines in a virtual machining system", Comput Aided Desi 45 (2013) 1306-1313.
[17] M. Soori, B. Arezoo, M. Habibi, "Tool deflection error of three-axis computer numerical control milling machines, monitoring and minimizing by a virtual machining system", J Manuf Sci Eng 138 (2016).
[18] M. Soori, M. Asmael, D. Solyalı, "Recent Development in Friction Stir Welding Process: A Review", SAE Int J Mater Manuf (2020) 18.
[19] M. Soori, M. Asmael, "Mechanical behavior of materials in metal cutting operations, a review", J New Technol Mater 10 (2020) 79-82.
[20] M. Soori, B. Arezoo, "Virtual Machining Systems for CNC Milling and Turning Machine Tools: A Review", Int J Eng Future Technol 18 (2020) 56-104.
[21] M. Soori, M. Asmael, "Virtual Minimization of Residual Stress and Deflection Error in Five-Axis Milling of Turbine Blades", Strojniski Vestnik/J Mech Eng 67 (2021) 235-244.
[22] Y. Altintas, P. Kersting, D. Biermann, E. Budak, B. Denkena, I. Lazoglu, "Virtual process systems for part machining operations", CIRP Annals 63 (2014) 585-605.
[23] Y. Zhao, J. Sun, J. Li, Y. Yan, P. Wang, "A comparative study on Johnson-Cook and modified Johnson-Cook constitutive material model to predict the dynamic behavior laser additive manufacturing FeCr alloy", J Alloys Compoun 723 (2017) 179-187.
[24] S.R. De Galarreta, J.R. Jeffers, S. Ghouse, "A validated finite element analysis procedure for porous structures", Mater & Desi 189 (2020) 108546.
[25] U. Karaguzel, U. Olgun, E. Uysal, E. Budak, M. Bakkal, "Increasing tool life in machining of difficult-to-cut materials using nonconventional turning processes", Int J Adv Manuf Technol 77 (2015) 1993-2004.
[26] S. Engin, Y. Altintas, "Mechanics and dynamics of general milling cutters.: Part I: helical end mills", Int J Mach Tools Manuf 41 (2001) 2195-2212.
[27] H. Erdim, I. Lazoglu, B. Ozturk, "Feedrate scheduling strategies for free-form surfaces", Int J Mach Tools Manuf 46 (2006) 747-757.
[28] G. Yu¨ cesan, Y. Altıntas¸, "Prediction of ball end milling forces", (1996).
[29] C. Ji, Y. Li, X. Qin, Q. Zhao, D. Sun, Y. Jin, "3D FEM simulation of helical milling hole process for titanium alloy Ti-6Al-4V", Int J Adv Manuf Technol 81 (2015) 1733-1742.
[30] A. He, G. Xie, H. Zhang, X. Wang, "A comparative study on Johnson–Cook, modified Johnson–Cook and Arrhenius-type constitutive models to predict the high temperature flow stress in 20CrMo alloy steel", Mater & Desi (1980-2015) 52 (2013) 677-685.
[31] Y. Lin, X.-M. Chen, "A combined Johnson–Cook and Zerilli–Armstrong model for hot compressed typical high-strength alloy steel", Comput Mater Sci 49 (2010) 628-633.
[32] X. Wang, C. Huang, B. Zou, H. Liu, H. Zhu, "Dynamic behavior and a modified Johnson–Cook constitutive model of Inconel 718 at high strain rate and elevated temperature", J. Wang, Mater Sci Eng: A 580 (2013) 385-390.
[33] J. Ren, J. Cai, J. Zhou, K. Shi, X. Li, "Inverse determination of improved constitutive equation for cutting titanium alloy Ti-6Al-4V based on finite element analysis", Int J Adv Manuf Technol 97 (2018) 3671-3682.
[34] J. Wang, W.-G. Guo, P. Li, P. Zhou, "Modified Johnson-Cook description of wide temperature and strain rate measurements made on a nickel-base superalloy", Mater High Temper 34 (2017) 157-165.